Journal of Power Sources 233 (2013) 202–208

Contents lists available at SciVerse ScienceDirect

Journal of Power Sources

journal homepage: www.elsevier.com/locate/jpowsour

Porous poly (ether sulfone) membranes with tunable morphology: Fabrication and their application for vanadium flow battery

Yun Li [a,b], Huamin Zhang [a,**], Xianfeng Li [a,*], Hongzhang Zhang [a,b], Wenping Wei [a,b]

[a] Division of energy storage, Dalian Institute of Chemical Physics, Chinese Academy of Sciences, Dalian 116023, PR China
[b] Graduate University of the Chinese Academy of Sciences, Beijing 100039, PR China

HIGHLIGHTS

- PES porous membranes with tunable morphology were fabricated for VFB application.
- The morphology of PES membranes can be easily tuned via addition of PVP in solutions.
- The membranes performance in VFB can be optimized via adjusting their morphology.
- PES porous membranes show very good prospective usages in VFB.

ARTICLE INFO

Article history:
Received 20 July 2012
Received in revised form
15 November 2012
Accepted 16 January 2013
Available online 26 January 2013

Keywords:
Energy storage
Poly (ether sulfone)
Porous membranes
Vanadium flow battery

ABSTRACT

Poly (ether sulfone) (PES) porous membranes with tunable morphology are prepared via phase inversion method and first investigated in vanadium flow battery (VFB) application. The morphology of PES membranes is adjusted via introducing hydrophilic poly (vinyl pyrrolidone) (PVP) in PES cast solutions. The effect of PVP (content, molecular weight) on the membranes morphology as well as their performance in VFB is studied in detail. The results show that: the addition of PVP in cast solutions could induce membranes with more porous structures and bigger pore size distribution. Therefore under VFB operating condition, the membranes show lower area resistance and higher ions permeability. As a result, the VFBs fabricated with the membranes show relatively higher voltage efficiency and lower coulombic efficiency. Thus the membranes with controlled performance in VFB can be realized via adjusting their morphology. This paper provides an effective way to optimize fabrication parameters of porous membranes for VFB application.

1. Introduction

Implementations of wind and solar energy generation have rapidly expanded around the world with the concerns of serious energy scarcity and environment pollution. However, the random and intermittent nature of these renewable sources makes it quite challenging to use and dispatch electricity through the grid. One effective solution is to connect the power station and the grid with energy storage systems. As one kind of electrochemical energy storage techniques, vanadium flow battery (VFB) becomes one of the ideal candidates for large scale energy storage due to its features like flexible design, high efficiency and long cycle life [1,2].

Normally a VFB single cell consists of two reservoirs containing active species of vanadium ions with different valence states, a battery cell and two pumps. As a key part of VFB cell, a membrane is employed to separate electrolytes (vanadium ions), while still transfer protons to complete the current circuit [3]. Therefore, an ideal membrane for VFB should meet the requirements of low vanadium permeability, high ion conductivity, excellent chemical and mechanical stability as well as low cost [4].

The currently used membranes in VFB are perflurosulfonic polymers such as DuPont Nafion®. Although the Nafion® membranes illustrate both high proton conductivity and chemical stability, the extremely high cost and low ion selectivity of these membranes (high vanadium crossover) have limited VFB commercialization [5]. Other types of commercial membranes, e.g. anionic Selemion AMV, DMV cationic Selemion CMV and microporous Daramic, were proved to be unsuitable for VFB application due to their poor chemical stability or ion selectivity [6,7]. Thus urgent need was brought to develop substitute membranes for VFB

* Corresponding author. Tel.: +86 41184379669; fax: +86 41184665057.
** Corresponding author.
E-mail addresses: zhanghm@dicp.ac.cn (H. Zhang), lixianfeng@dicp.ac.cn (X. Li).

0378-7753/$ – see front matter © 2013 Elsevier B.V. All rights reserved.
http://dx.doi.org/10.1016/j.jpowsour.2013.01.088

application. Recently, porous nanofiltration (NF) membrane separators were successfully applied in VFB based on the idea of tuning V/H selectivity via pore size exclusion [8]. This totally new idea successfully overcomes the restriction caused by ion exchange groups from traditional ion exchange membranes and provides a new way to fabricate high performance VFB separator [9]. The NF membranes could separate vanadium ions (V(II), V(III), V(IV), and V(V)) from protons due to their difference in radius, charge density and further realize their application in VFB.

The research of NF membrane separator in VFB application was just started. Plenty of factors could affect their performance in VFB. Among all the factors, the morphology of membranes could be one of the most important roles in determining their final performance in VFB. Apparently, the morphology of NF membranes could be controlled by different factors, especially the preparation parameters, e.g. the concentration, the additives, the precipitation bath, etc. [10–12].

Poly (ether sulfone) has been widely used as membrane material for the applications of ultrafiltration, microfiltration and nanofiltration due to its excellent chemical and mechanical stability. PES membranes prepared by phase inversion normally possess an asymmetric structure including a skin layer and a porous support layer. The membrane morphology could be effectively and conveniently controlled by adding a third component to the cast solutions, such as low molecular weight additives (e.g. LiCl, $LiClO_4$) [13,14] and polymeric components (e.g. polyethylene glycol (PEG), polyvinylpyrrolidone (PVP)) [15,16]. Among the additives, PVP has been widely exploited, due to its good miscibility with PES and high solubility in non-solvent. For example, Matsuura et al. [17] studied the effect of PVP on the performance of polyethersulfone ultrafiltration membranes. They concluded that the strong interaction between PVP and polysulfone caused an increase in the pore size and consequently improved the permeation rate. Compared with the traditional ternary system (PES/solvent/non-solvent), the additive could change the composition path during the phase inversion process. Since the equilibrium binodal of the quaternary system PES/PVP/solvent/non-solvent lies inside the demixing gap rather than outside the ternary system, instantaneous demixing occurs after immersion [18,19].

To clarify the role of additives in membrane formation and to further know their effect on the membrane morphology and their performance in VFB, a series of asymmetric PES membranes with different pore size distribution were prepared by controlling the content and the molecular weight of PVP in the cast solutions. Their morphology together with performance were investigated in detail, which will give more choices to further control the final membrane properties. The relationship between membranes morphology and their performance in VFB will be established, which will provide an effective way to fabricate high performance porous membranes with tuned morphology for VFB application.

2. Experimental

2.1. Materials

Polyethersulfone (PES) was obtained from Changchun Jilin University Special Plastic Engineering Research, with viscosity of 0.58. PVPs with molecular weight of 10,000, 58,000, and 1,300,000 (referred as to PVP10, PVP58, and PVP130 respectively) were used as pore-forming materials.

2.2. Membrane preparation

The PES membranes were prepared by phase inversion technique from a solution containing certain weight ratio of PES and PVP dissolved in *N*,*N*-dimethylacetamide. Then the solution was cast on a clean glass plate at room temperature with humidity less than 40% to avoid the penetration of water vapor into the polymer solution. After evaporation for 10 s, the plate was immersed in water to form the membranes. The detailed composition of resulted membranes was shown in Tables 1 and 2.

Table 1
Physicochemical properties of PES membranes with different proportions of PVP.

Membrane	Proportion (PES/PVP[a]/DMAc)	Thickness (μm)	Area resistance (Ω cm^2)
M0	1/0/2	115(±5)	277.40
M1	1/0.18/2	115(±5)	4.70
M2	1/0.25/2	115(±5)	2.74
M3	1/0.33/2	115(±5)	0.77
M4	1/0.43/2	115(±5)	0.35
M5	1/0.54/2	115(±5)	0.18

[a] PVP with molecular weight of 10,000.

2.3. Membrane characterization

2.3.1. Scanning electronic microscopy (SEM) and field emission scanning electronic microscopy (FE-SEM)

The cross-section and surface morphology of the membranes were investigated by SEM (JEOL 6360LV, Japan) and FE-SEM (QUANTA 200FEG). The samples prepared for cross-section morphology observation were obtained by breaking the membranes in liquid nitrogen and coating them with gold before measurement.

2.3.2. Area resistance

The area resistance of the membranes was detected with the method described in our previous article [20]. Two cuboid half cells containing 0.5 M H_2SO_4 were separated by the membrane. The effective area of the cell was designed as 1 cm^2. r_1 and r_2, which represent the electric resistances of the cell with and without a membrane respectively were determined by electrochemical impedance spectroscopy (EIS) over a frequency range from 1 kHz to 1 MHz, the area resistance r was calculated by Eq. (1):

$$r = (r_1 - r_2) \times S \tag{1}$$

2.3.3. Vanadium/proton permeability

The permeability of vanadium ions with different valences through a membrane was determined with diffusion cells reported elsewhere [21]. The effective area of the membranes was 9 cm^2. The right cell was filled with 75 ml 1.5 M $MgSO_4$ in 3 M H_2SO_4 aqueous solution to equalize the ionic strengths and minimize the osmotic pressure effect. And the left one was filled with 75 ml electrolyte containing vanadium ions with different valence states ($V^{3+}/VO^{2+}/VO_2^+$) which correspond to $V^{3+}/VO^{2+}/VO_2^+$ permeability respectively. Magnetic stirrers were utilized to eliminate the concentration polarization. Samples from the right cell were collected at regular time intervals. The concentration of VO^{2+} was measured by UV–vis spectrometer, while the concentration of V^{3+}/VO_2^+ was detected by automatic potentiometric titration

Table 2
Physicochemical properties and performance of PES membranes with different molecular weights of PVP.

Membrane	Proportion (PES/PVP/DMAc)	Molecular weight of PVP	Thickness (μm)	CE (%)	EE (%)	VE (%)
M6	1/0.25/2	10,000	115(±5)	96.67	70.16	72.58
M7	1/0.25/2	58,000	115(±5)	97.03	68.60	70.71
M8	1/0.25/2	1,300,000	115(±5)	96.53	69.28	71.18

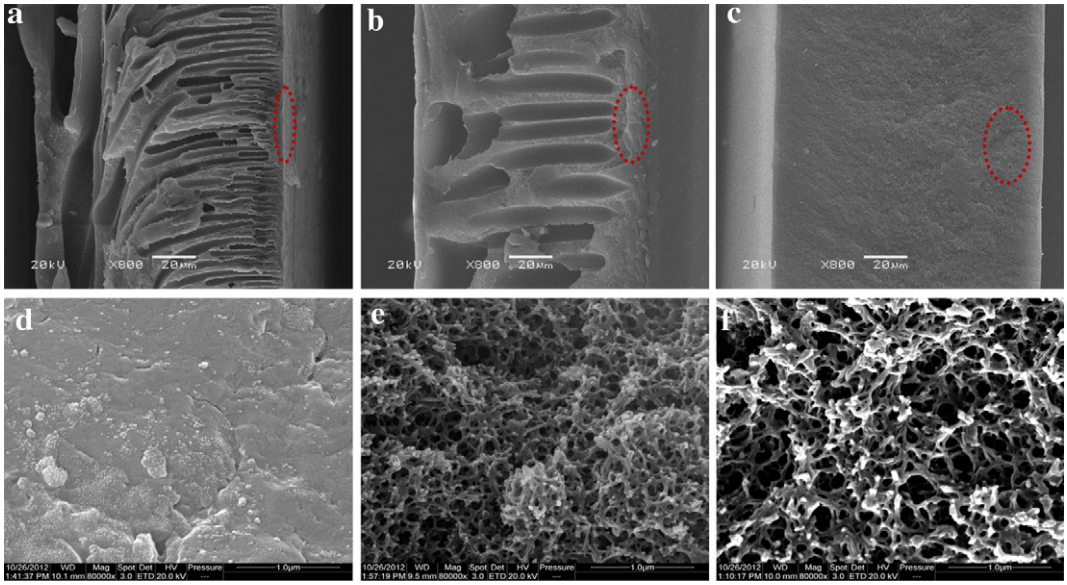

Fig. 1. Cross-section morphology of PES membranes (a: M1, b: M3, c: M5) and corresponding morphology of skin layers (d: M1, e: M3, f: M5).

instrument. The vanadium permeability was calculated according to the Ficker diffusion law as follows:

$$V_B \frac{dC_B(t)}{dt} = A\frac{P}{L}(C_A - C_B(t)) \quad (2)$$

where V_B is the solution volume in the deficiency side; A and L are the effective area and thickness of the membrane, respectively; P is the permeability of vanadium ion; C_A is vanadium ions concentration in enrichment side, C_B is vanadium ions concentration in deficiency side.

The device used for measuring the permeability of protons is similar to that of vanadium, except that the right cell filled with deionized water and the concentration of H^+ was characterized by Mettler Toledo pH meter.

2.3.4. VFB single cell performance

A VFB single cell was assembled by sandwiching a membrane with two carbon felt electrodes, clamped by two graphite polar plates. All these components were fixed between two stainless plates. 30 ml 1.5 M V^{2+}/V^{3+} in 3.0 M H_2SO_4 and 30 ml 1.5 M VO^{2+}/VO_2^+ in 3.0 M H_2SO_4 solutions were used as negative and positive electrolytes respectively. The electrolyte was cyclically pumped through the corresponding electrodes in airtight pipe lines. Charge–discharge cycling tests were conducted by Arbin BT2000 with a constant current density of 80 mA cm^{-2}. The cut-off voltage for charge and discharge was set at 1.65 V and 0.8 V respectively to avoid the corrosion of carbon felts and graphite polar plates.

2.3.5. Self-discharge test

The VFB battery was assembled as mentioned in Section 2.3.4. Self-discharge began at the state of charge (SOC) of 50% and stopped until the voltage dropped below 0.8 V.

2.3.6. Stability test

The chemical stability of membranes was investigated according to the method reported by Kim et al. [22,23]. A 3 cm × 3 cm PES membrane sample was immersed 60 mL electrolyte solution (0.15 M VO_2^+ in 3 M total sulfate) at 40 °C. During test, a 2 mL electrolyte sample was collected from the bottle at a regular time interval. VO^{2+} concentration in the testing solution was recorded as an indicator of membrane oxidation degradation.

To further investigate the oxidation stability of PES membranes, the charge–discharge cycling life test was carried out at a constant current density of 80 mA cm^{-2}.

3. Results and discussion

3.1. Morphology

SEM was utilized to investigate the morphology of the prepared membranes. The cross-section in Fig. 1(a–c) demonstrates that the

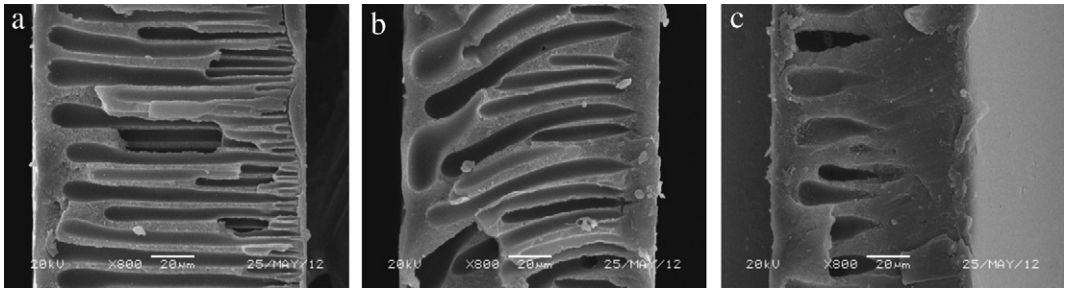

Fig. 2. Cross-section morphology of membranes (a: M6, b: M7, c: M8).

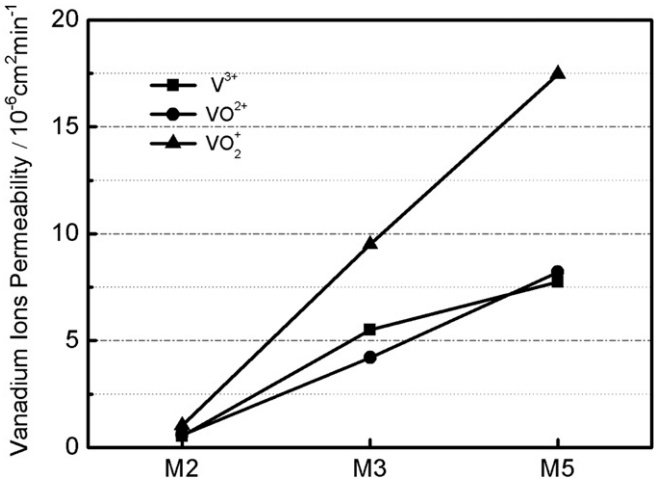

Fig. 3. Vanadium ions permeability of M2/M3/M5 membranes.

distance from the top surface to the starting point of the macrovoid formation increases with the proportion of PVP increasing from 0.18 to 0.54, while, their sublayers vary from finger like to sponge like pores. Fig. 2 indicates that the similar trend of top layer appears with increasing PVP molecular weight. Compared with M6 and M7, the skin layer of M8 becomes thicker when PVP130 with the highest molecular weight was added into a cast solution.

Normally, PVP in a cast solution causes thermodynamic enhancement and kinetic hindrance during phase separation process [15], since it plays the role of reducing the miscibility of casting solutions with non-solvent as well as increasing the solution viscosity. Apparently, the kinetic hindrance dominates the phase inversion process in this system. The viscosity of the casting solution hampers the exchange between solvent and non-solvent during the demixing process. Hence, a relatively thicker skin layer forms with higher PVP proportion or higher molecular weight. In addition, during macrovoid formation, a skin layer could hinder the penetration of non-solvent into the sublayer. In other words, this skin layer limits the nuclei formation after a few nuclei, which are benefit for macrovoid development. As PVP content increasing, the pore size of skin layer could be too large to retain solvent, thus plenty of nuclei will be formed and finally result in a sponge type structure [24].

Besides, the magnified skin layer structure of M1 M3 and M5 in Fig. 1(d–f), indicated that the pore size of the skin layer becomes larger and more interconnected with increasing PVP proportion, which well agrees with previous report [12]. Compared with higher molecular weight PVP, lower molecular weight PVP tends to form smaller pores and easily leaches out from the membrane. However, during membrane forming process, high molecular weight PVP possibly remains in the membrane and blocks the interconnected pores [15,25].

3.2. Vanadium/proton permeability

To further link the membranes morphology described above with their selectivity, the permeability of vanadium ions with different valence states through the membranes was detected and listed in Fig. 3. As expected, with the PVP content increasing, the permeability of $V^{3+}/VO^{2+}/VO_2^+$ increases due to their larger pore size and interconnected distribution. For example, the V^{3+} permeability varies from 0.53×10^{-7} cm^2 min^{-1} to 7.75×10^{-7} cm^2 min^{-1} with the proportion of PVP increasing from 0.18 to 0.54, while the permeability of VO^{2+} is in between 0.58×10^{-7} cm^2 min^{-1} and 8.20×10^{-7} cm^2 min^{-1}. As discussed above, the skin layer of membranes gets thicker and more porous with the addition of PVP in cast solutions. It seems that the pore size exclusion overweighs the thickness of skin layer on preventing the vanadium ions through membranes. To note that: PES membranes prepared from the solutions without addition of PVP (M0) show too low permeability to be detected due to its disconnected porous structures. As for all membranes, taking M2 for example, the VO_2^+ permeability is almost twice that of V^{3+} and VO^{2+}. It shows the similar trend as M3 and M5. It's well known that the vanadium species exhibit a rich aqueous chemistry, where their existence forms strongly depend on the pH and concentration of electrolyte. It is supposed that V^{3+} and VO^{2+} species exist as $[V(H_2O)_6]^{3+}$ and $[VO(H_2O)_5]^{2+}$, however, even more complicated with various pH and concentrations [26,27]. A recent research reported that VO_2^+ species exist as $[VO_2(H_2O)_3]^+$ in concentrated sulfuric acid solutions [28,29]. Considering the different steric hindrances through the pores with respect to different hydrated vanadium species, the VO_2^+ species bonding with the least water molecules possibly transport more easily through the membranes.

The linear relationship between VO^{2+}/H^+ concentration in the deficiency side and diffusion time is illustrated in Fig. 4. The slope reflects the permeability of VO^{2+} and H^+ through membranes with various PVP contents. The slope of the line increases from M1 to M5 indicating the increased pore size and interconnected pores distribution with increasing PVP content in cast solutions. Compared with vanadium ions, protons transport much faster for all the membranes. In the practical application, membrane morphology should be carefully adjusted to balance vanadium ions prevention and protons transportation, since too large pores will lead to

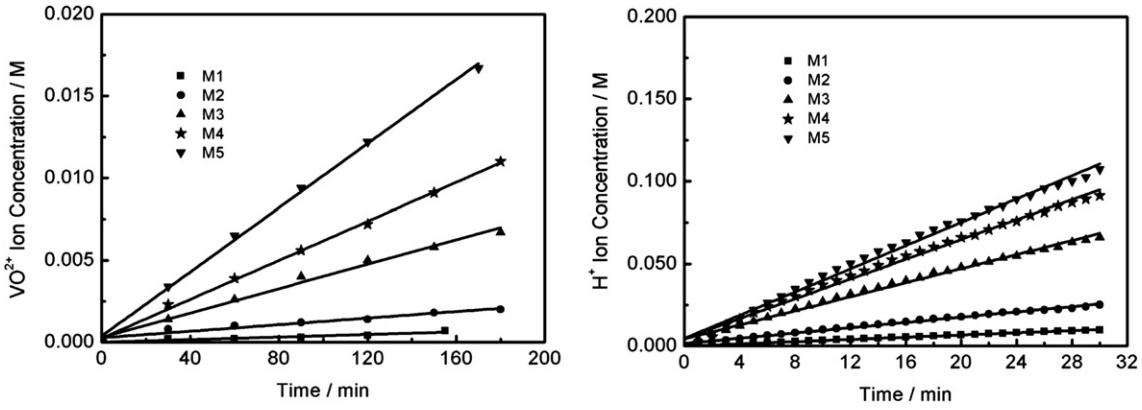

Fig. 4. VO^{2+} and H^+ concentrations in the deficiency side of the permeation measuring device with M1–M5 membranes.

electrolytes cross-mix, while too small pores will induce too high resistance to protons.

3.3. Area resistance

As listed in Table 1, the area resistance decreases from 4.70 Ω cm^2 to 0.18 Ω cm^2 sharply from M1 to M5. For PES membranes, the lean phase and rich phase of the continuous PES intertwine each other and form interconnected winding pores. The pores were filled with H_2SO_4 before measurement by soaking the membranes in H_2SO_4 solutions. The protons afford less restriction with pore size increasing. For example, as for M5, the pore size is too large to retain protons thus the protons can go through the channels "freely". However, the vanadium permeability boosts as well. For membranes prepared without addition of PVP (M0), the area resistance is much higher than other membranes due to their smaller pore size and disconnected pore distribution. All these results are well in agreement with the results of morphology and ion permeability described above.

3.4. Single cell performance

Fig. 5 demonstrates the VFB single cell performance assembled with M0–M5 membranes. M0 and M1 possess too high area resistance, so the VFBs assembled with them exhibit too high ohmic overpotential and can't complete the charge–discharge process. With proportion of PVP increasing, the coulombic efficiency (CE) declines from 95.6% to 66.8% and the voltage efficiency (VE) rises gradually from 69.6% to 85.9% then drops to 81.6%. While the energy efficiency (EE) first reaches a peak at 76.1% then decreases to 54.6%.

The coulombic efficiency (CE) is defined as the ratio of a cell's discharge capacity (Q_{dis}) divided by its charge capacity (Q_{cha}) under certain charge–discharge conditions. The higher CE, indicating lower capacity loss, is mainly attributed to the lower rate of cross-mixed vanadium ions. The result is in accordance with vanadium permeability. With increasing proportion of PVP in cast solution, their morphology becomes more porous and well interconnected, as a result, ions permeability increases and vanadium ions partly cross-mix, therefore lower CE (Fig. 5). The voltage efficiency (VE) is related to the internal resistance of battery. Higher VE means higher proton permeability or lower battery resistance. With increasing content of PVP in cast solutions, the area resistance of membranes (M2–M4) decreases, accordingly, their VE increases from 69.6% to 85.9%. As for M5, the membrane structure is too open

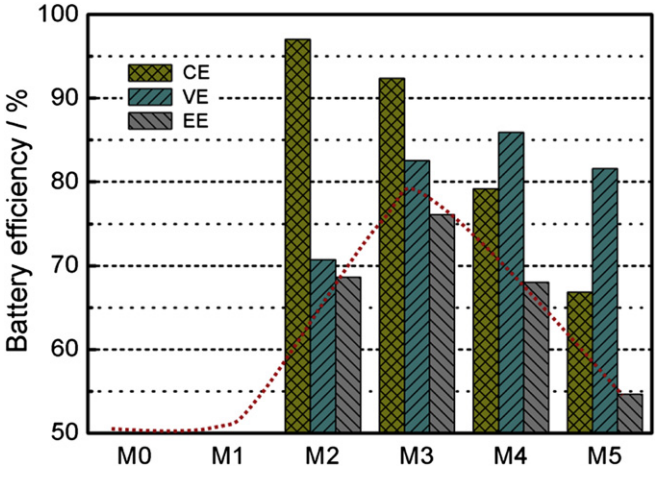

Fig. 5. VFB efficiency assembled with M0–M5 membranes under the charge–discharge current density of 80 mA cm^{-2}.

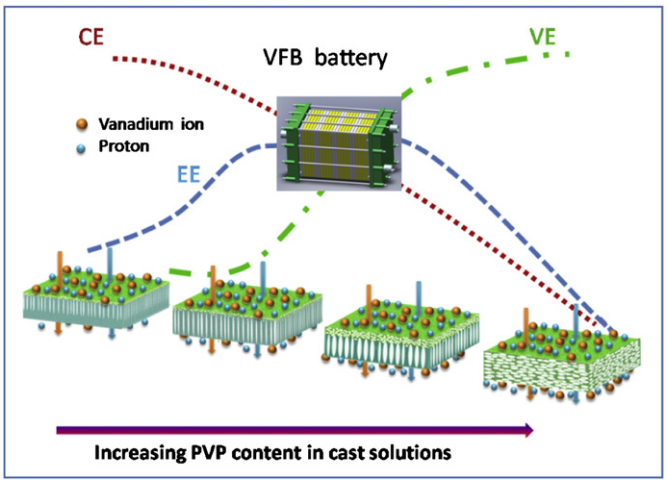

Fig. 6. Schematic of PES membranes with variational cross-section morphology.

to retain any ions including protons and vanadium ions, as a result, the CE is very low due to the ion cross-mixing so as the VE. Therefore a balance between ion selectivity and proton conductivity should be made via optimize the membrane morphology and their performance in VFB (Fig. 6). The energy efficiency (EE) is a very important indicator, which reflects the energy conversion ability of for large scale energy storage devices. As expected, the energy efficiency of the VFB assembled with prepared membranes first increases then decreases with increasing content of PVP in cast solutions. In this system, M3 with 9.91 wt.% of PVP shows the best performance of CE 92.4% and EE 76.1%, which is comparable with our reported PAN-H NF membranes [8]. Moreover, as one type of thermal plastics, PES membranes show excellent chemical stability, since it truly does not carry any ion exchange groups.

Table 2 shows the performance of the VFB assembled with membranes prepared from solutions with addition of different MW PVP. To our surprise, all the membranes illustrate similar performance, even though they carry different morphology. Their CE fluctuates between 96% and 97%, while the VE fluctuates around 71%. As discussed above, the addition of PVP with high molecular weight could increase the pore size and porosity of the top layer, however possibly could block interconnected pores as well. It seems that the two contradictory aspects trade off and take turns, which further affect the vanadium/proton permeability. Therefore it's reasonable that the VFB with M6–M8 membranes show similar CE and VE.

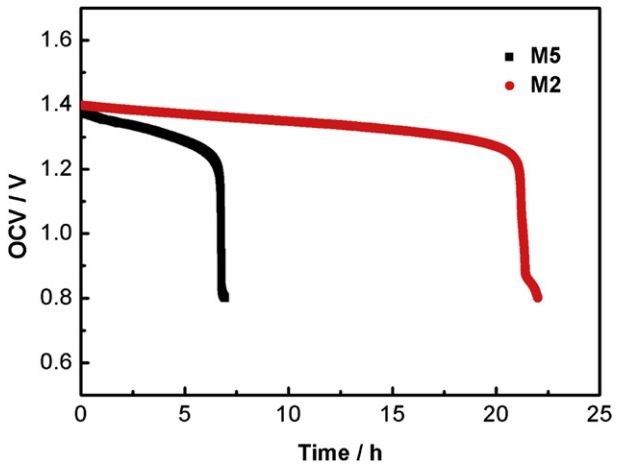

Fig. 7. OCV decay curves of the VFB cell with M2 and M5 membranes.

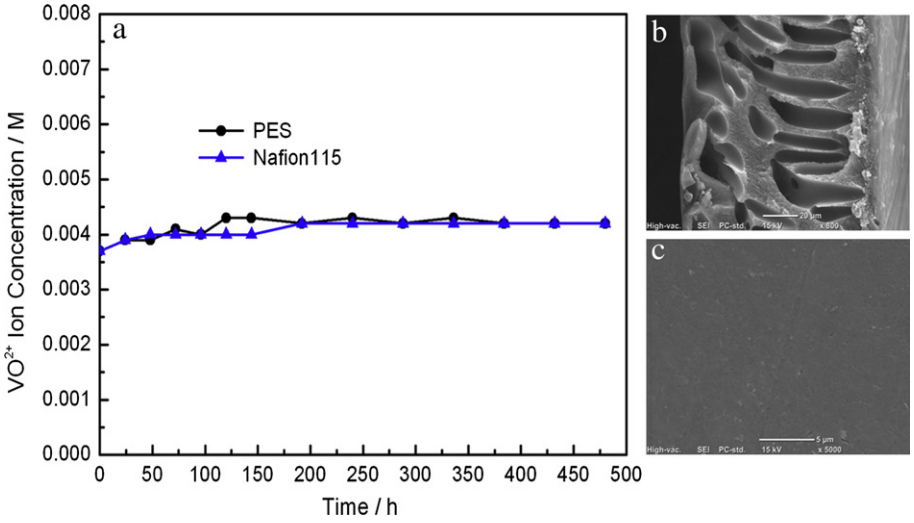

Fig. 8. Chemical stability of PES membranes: (a) VO^{2+} concentration change of electrolyte solution (0.15 M VO_2^+ in 3 M total sulfate) involving PES membrane M3 and Nafion 115 as function of time; (b) and (c) cross-section and surface morphology of M3 membrane after 20 days.

3.5. OCV test

Open circuit voltage (OCV) of the VFB was monitored at room temperature after it was charged to a 50% state of charge (SOC) and was presented in Fig. 7. It can be seen that the OCV value marginally declines with storage time prolonging at initial phase and then drops rapidly to 0.8 V. The maintaining time of OCV above 1.0 V of the VFB assembled with M2 membrane is about 22 h, which is roughly two times longer than that of the VFB assembled with M5 membrane. This reveals that the rate of self-discharge of the VFB with M2 membrane is much slower than that of the VFB with M5 membrane. The results well agree with their morphology tendency.

3.6. The oxidation stability and cycle life of PES membranes

Fig. 8a exhibits the VO^{2+} concentration variation in electrolyte solution in which PES porous membrane and Nafion 115 were immersed for 20 days at 40 °C. In terms of the solution containing PES membrane, the VO^{2+} concentration barely changed compared with blank solution during the whole stage, as well as the solution containing Nafion 115, indicating that the prepared PES membranes are highly stable in VO_2^+ solution. The morphology of PES membranes after treatment was investigated by SEM (Fig. 8b and c). The PES membrane showed a relatively smooth surface and no cracks were observed after treatment. The cross section structure did not change obviously compared with that of the initial membrane as well (Fig. 1).

The cycle life of VFB assembled with M3 was carried out at the current density of 80 mA cm^{-2}. As shown in Fig. 9a, the CE of the VFB remains stable at around 92% over 150 cycles and the VE of the VFB fluctuates between 82% and 85%, which demonstrates that there is no fouling of the membrane, which could lead to blockage of the pores and reduced transfer rates of ions across the membrane. SEM was carried out on the membranes before and after VFB test to further investigate the membrane stability (Fig. 9c). Except for some dents resulting from compressed carbon felts, the membrane surface still kept smooth after test (Fig. 9c). Moreover, no

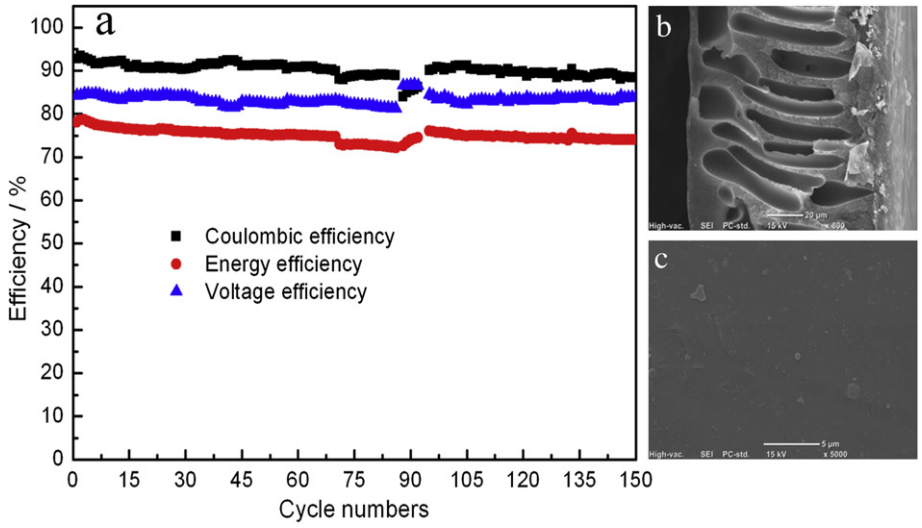

Fig. 9. Cycle life performance of M3 membrane in VFB operation: (a) charge–discharge cycling performance of VFB assembled with M3 membrane at 80 mA cm^{-2}; (b) and (c) cross-section and surface morphology of M3 after test.

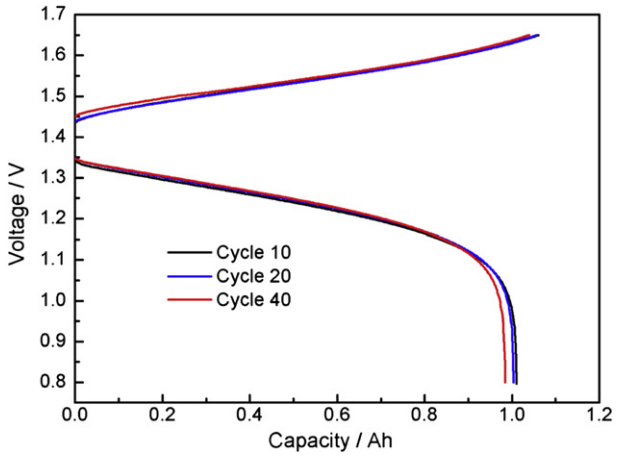

Fig. 10. Charge and discharge curves of membrane M2 membrane in VFB operation (80 mA cm^{-2}) with different cycles.

collapse of pores in sublayers occurred as shown in Fig. 9b after cycle test. As described above, the EE which reflects comprehensive performance of VFB kept stable as well over 150 cycles and there is no remarkable decay of capacity after the cell running for 10, 20, 40 cycles (Fig. 10). Overall, cycle performance of VFB single cell illustrates that PES porous membranes own high chemical and mechanical stability in VFB operation and thus are able to maintain cell capacity and performance.

4. Conclusions

In this work, PES membranes with different morphology were prepared by introducing hydrophilic PVP additives in the casting solution. The cross-section and surface morphology of the membranes were characterized via SEM and FE-SEM respectively. With addition of PVP in the cast solutions, the cross-section morphology tuned from asymmetric finger like pores to sponge like pores. The pores of the selective layer became bigger and more interconnective with increasing content of PVP, as a result, higher permeability for both vanadium ions and protons in VFB application. The performance of VFB assembled with these membranes first increased then decreased due to the balance between membranes selectivity and ion conductivity. The VFB assembled with PES membranes with optimized morphology showed CE of 92.4% and EE of 76.1% at current density of 80 mA cm^2, which was comparable with previous reported NF membranes. The VFB cell assembled with PES porous membrane exhibited stable performance during 150 cycles. Therefore, PES membranes with proper morphology show quite good potential usage in VFB.

Acknowledgments

The authors acknowledge the financial support from National Basic Research Program of China (973 program No. 2010CB227202), China Natural Science Foundation (No. 21206158) and Youth Innovation Promotion Association of CAS.

References

[1] M. Skyllas-Kazacos, M.H. Chakrabarti, S.A. Hajimolana, F.S. Mjalli, M. Saleem, Journal of The Electrochemical Society 158 (2011) R55–R79.
[2] Z. Yang, J. Zhang, M.C.W. Kintner-Meyer, X. Lu, D. Choi, J.P. Lemmon, J. Liu, Chemical Reviews 111 (2011) 3577–3613.
[3] X. Li, H. Zhang, Z. Mai, H. Zhang, I. Vankelecom, Energy & Environmental Science 4 (2011) 1147–1160.
[4] B. Schwenzer, J. Zhang, S. Kim, L. Li, J. Liu, Z. Yang, ChemSusChem 4 (2011) 1388–1406.
[5] T. Sukkar, M. Skyllas-Kazacos, Journal of Applied Electrochemistry 34 (2004) 137–145.
[6] T. Mohammadi, M. Skyllas-Kazacos, Journal of Applied Electrochemistry 27 (1996) 153–160.
[7] B. Tian, C.-W. Yan, F.-H. Wang, Journal of Applied Electrochemistry 34 (2004) 1205–1210.
[8] H. Zhang, H. Zhang, X. Li, Z. Mai, J. Zhang, Energy & Environmental Science 4 (2011) 1676–1679.
[9] X. Li, S. De Feyter, D. Chen, S. Aldea, P. Vandezande, F. Du Prez, I.F.J. Vankelecom, Chemistry of Materials 20 (2008) 3876–3883.
[10] J.R. Hwang, S.-H. Koo, J.-H. Kim, A. Hicuchi, T.-M. Tak, Journal of Applied Polymer Science 60 (1996) 1343–1348.
[11] P.S.T. Machado, A.C. Habert, C.P. Borges, Journal of Membrane Science (1999) 171–183.
[12] P. van de Witte, P.J. Dijkstra, J.W.A. van den Berg, J. Feijen, Journal of Membrane Science 117 (1996) 1–31.
[13] D.L. Wang, K. Li, W.K. Teo, Journal of Membrane Science 178 (2000) 13–23.
[14] M.L. Yeow, Y.T. Liu, K. Li, Journal of Membrane Science 258 (2005) 16–22.
[15] J.-H. Kim, K.-H. Lee, Journal of Membrane Science 138 (1997) 153–163.
[16] S.H. Yoo, J.H. Kim, J.Y. Jho, J. Won, Y.S. Kang, Journal of Membrane Science 236 (2004) 203–207.
[17] L.Y. Lafreniere, F.D.F. Talbot, T. Matsuura, S. Sourirajan, Industrial & Engineering Chemistry Research 26 (1987) 2385–2389.
[18] I.M. Wienk, R.M. Boom, M.A.M. Beerlage, A.M.W. Bulte, C.A. Smolders, H. Strathmann, Journal of Membrane Science 113 (1996) 361–371.
[19] R.M. Boom, T. Boomgaard, C.A. Smolders, Journal of Membrane Science 90 (1994) 231–249.
[20] Z.S. Mai, H.M. Zhang, X.F. Li, C. Bi, H. Dai, Journal of Power Sources 196 (2011) 482–487.
[21] Q. Luo, H. Zhang, J. Chen, D. You, C. Sun, Y. Zhang, Journal of Membrane Science 325 (2008) 553–558.
[22] S. Kim, T.B. Tighe, B. Schwenzer, J. Yan, J. Zhang, J. Liu, Z. Yang, M.A. Hickner, Journal of Applied Electrochemistry 41 (2011) 1201–1213.
[23] C. Fujimoto, S. Kim, R. Stains, X. Wei, L. Li, Z.G. Yang, Electrochemistry Communications 20 (2012) 48–51.
[24] H. Matsuyama, T. Maki, M. Teramoto, K. Kobayashi, Separation Science and Technology 38 (2003) 3449–3458.
[25] D.L. Wang, K. Li, W.K. Teo, Journal of Membrane Science 163 (1999) 211–220.
[26] K. Kanamori, Coordination Chemistry Reviews 237 (2003) 147–161.
[27] M. Vijayakumar, S.D. Burton, C. Huang, L. Li, Z. Yang, G.L. Graff, J. Liu, J. Hu, M. Skyllas-Kazacos, Journal of Power Sources 195 (2010) 7709–7717.
[28] M. Vijayakumar, L. Li, G. Graff, J. Liu, H. Zhang, Z. Yang, J.Z. Hu, Journal of Power Sources 196 (2011) 3669–3672.
[29] L. Li, S. Kim, W. Wang, M. Vijayakumar, Z. Nie, B. Chen, J. Zhang, G. Xia, J. Hu, G. Graff, J. Liu, Z. Yang, Advanced Energy Materials 1 (2011) 394–400.